

Polypropylene–rubber blends: 5. Deformation mechanism during fracture

A. van der Wal¹, R.J. Gaymans*

Laboratory of Polymer Technology, Department of Chemical Technology, Twente University, P.O. Box 217, NL-7500 AE, Enschede, The Netherlands

Received 29 May 1997; received in revised form 9 February 1998; accepted 6 May 1998

Abstract

The deformation mechanism of polypropylene–EPDM rubber blends during fracture was studied by post-mortem SEM fractography. The deformation mechanism was determined for various blend morphologies and test conditions. Brittle fracture merely gives rise to voids, which are caused by voiding of the rubber particles. In the case of ductile fracture, voiding of rubber particles and strong shear yielding of the matrix takes place. In this yielding process these voids become elongated. As the fracture surface is approached the voids are more deformed. At high test speed, in ductile fracture, along the fracture surface a layer is formed without deformation. The thickness of this layer is 10–100 μm . This layer without deformation indicates that during deformation relaxation of the matrix material in this layer has taken place. With the formation of the relaxation layer the impact energy increases. The relaxation layer has thus a blunting effect. If a blend with large EPDM particles (1.6 μm) is deformed, in the rubber particles now several cavities are formed and these cavities are positioned near the interface with the matrix. It can be expected that it is an advantage to have several small cavities instead of one large cavity. The polypropylene matrix was found to deform by a shear yielding mechanism and multiple crazing was not observed. © 1999 Elsevier Science Ltd. All rights reserved.

Keywords: Polypropylene–rubber blends; Deformation mechanism; Melt layer

1. Introduction

The impact strength of a polymer may be improved by incorporation of a dispersed rubber phase. Polypropylene–rubber (PP–rubber) blends are very ductile materials [1–8]. At high temperatures they fracture in a ductile manner and have a very high fracture energy and at low temperatures they fracture in a brittle manner. The temperature at which this brittle–ductile transition takes place is called the brittle–ductile transition temperature (T_{bd}). This transition temperature depends on matrix parameters [4], blend morphology [3,7] and test conditions [1,5,6]. The deformation proceeds differently below and above the brittle–ductile transition and also changes with test speed. The deformation mechanism of rubber-toughened PP is attributed to both multiple crazing and yielding. Ramsteiner [1] studied this deformation mechanism at -40°C for reactor blends. From TEM studies and dilatometry measurements he concluded that multiple crazing is the dominant mechanism. Hayashi et al. [2] demonstrated that crazing and yielding in PP–rubber blends may occur simultaneously. Jang et al. [3] found for PP–EPDM that the deformation mechanism depends on the particle size.

Particles larger than 0.5 μm initiates crazes, while those smaller than 0.5 μm initiate yielding. The deformation of PP–rubber blends is accompanied by stress whitening. The stress whitening is due to a cavitation process in the system.

Dijkstra et al. [10] studied the effect of the test speed on the deformation mechanism of rubber-toughened nylon in the case of tough fracture. The mechanism was studied by post-mortem SEM analysis of the fracture zone perpendicular to the fracture surface. At low test speed (10^{-3} m/s) (strain rate 2.8×10^{-3} s⁻¹) at some distance from the fracture surface more or less around voids were observed in the rubber particles. Voids encountered in the vicinity of the fracture surface have a more elongated shape. The layer containing voids is referred to as the cavitation layer; the layer with elongated voids as the deformation layer. With increasing test speed a third layer, the relaxation layer, appears just beneath the fracture surface [10,11]. No sign of deformation is observed within the relaxation layer. The absence of cavities is due to relaxation of the matrix material. As relaxation is a result of strong adiabatic plastic deformation [5,6]. The relaxation layer has in nylon-blends a thickness of 3–5 μm . The relaxation layer is observed in ABS too [12,13]. A similar layer is seen in PP–EPDM blends [6]. The temperature rise during fracture of rubber-toughened PP on sample surfaces was measured by infrared thermography [7]. The notched specimens were fractured

* Corresponding author.

¹ Present address: Resina Chemie, 9607 PS Foxhol, The Netherlands.

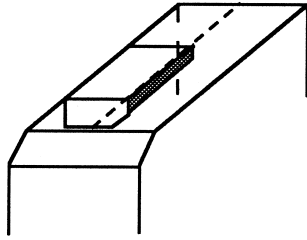


Fig. 1. Sample position. Micrographs refer to the shaded area.

using a tensile test. The temperature rise begins at a test speed of approximately 10^{-5} m s^{-1} (strain rate $2.8 \times 10^{-5} \text{ s}^{-1}$) and increases almost linearly with the logarithm of the test speed, from 30°C at 10^{-4} (strain rate $2.8 \times 10^{-4} \text{ s}^{-1}$) to around 90°C at 10 m/s (strain rate 28 s^{-1}). These values represent the specimen surface temperatures; the corresponding core temperatures are probably higher.

In this context, the deformation mechanism accompanying fracture of PP–rubber blends was investigated for various blend morphologies and test conditions. The stress whitening behaviour and the micro-deformation mechanisms were examined. The micro-deformation mechanisms were studied by post-mortem SEM fractography.

2. Experimental

The PP–EPDM blends were made by extrusion compounding and the test samples by injection moulding [6]. The specimens (ISO 180/1A, $74 \times 10 \times 4 \text{ mm}$) were injection moulded and a notch was milled in the specimens. The notched specimens were fractured by a tensile test, unless mentioned otherwise. This fracture test is referred to as a single-edge notch (SEN) tensile test and was carried out at different test speeds with a sample length between the clamps of 45 mm [6]. The test speed correlates with the apparent strain rates of the elastic part of the deformation as 1 m s^{-1} to 28 s^{-1} .

The deformation mechanism in the matrix was studied by post-mortem SEM analysis of the fracture zone in a plane perpendicular to the fracture surface and parallel to the crack propagation direction, as shown in Fig. 1. Samples for SEM were cut from the specimens with a fresh razor

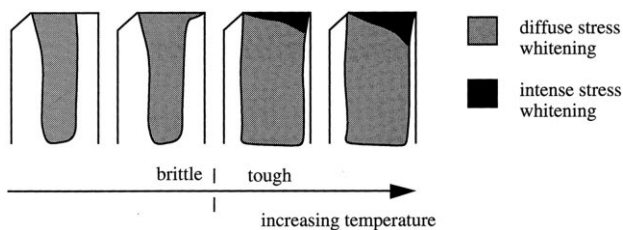


Fig. 2. Schematic representation of the evolution of the stress whitening with temperature in rubber-toughened polypropylene fractured during an SEN tensile test.

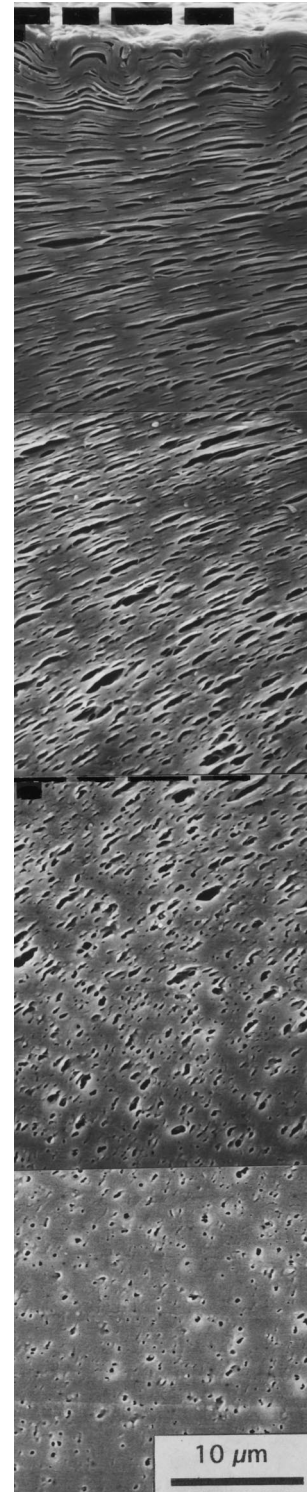


Fig. 3. Typical fracture zone of a tough fractured rubber-toughened polypropylene specimen at low test speed (10^{-3} m s^{-1}). The fracture surface is located at the top. The crack propagates from left to right.

blade, and then trimmed on a polishing machine to avoid deformation during trimming. The finishing preparation was carried out by cryotomography at -100°C with a diamond knife. The surface was sputter-coated with a

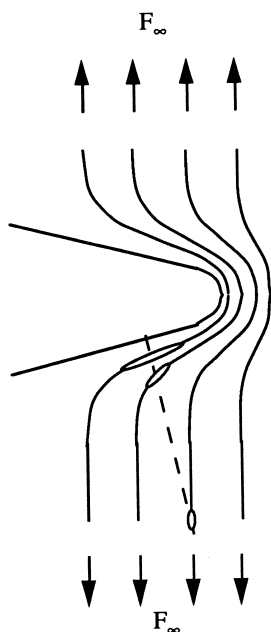


Fig. 4. Schematic representation of the force direction in the vicinity of a crack tip.

thin gold layer and studied using a Hitachi S-800 field emission SEM.

3. Results and discussion

3.1. Ductile fracture

Matrix deformation during fracture of rubber-toughened materials is accompanied by stress whitening. This stress whitening illustrates the deformation mechanism on a macroscopic scale. The development of the stress whitening in rubber-toughened PP with respect to temperature is schematically represented in Fig. 2. The specimens were fractured by an SEN tensile test. Stress whitening becomes visible above the glass transition temperature of the rubber phase.

Prior to the brittle–ductile transition, diffuse stress whitening is observed over the entire length of the specimen. In the case of tough fracture a triangular shaped zone of intense stress whitening appears at the fracture zone, surrounded by diffuse stress whitening. There is a clear demarcation between sections showing intense and diffuse stress whitening. The thickness of the intense stress whitening zone increases with increasing distance from the notch and with increasing temperature. The maximum thickness of the thickest part of the zone of intense stress whitening is at least 10 mm. Diffuse stress whitening is restricted to the core of the specimen, the material adjacent to the free surfaces remained transparent.

The studied fracture zone is located at the notch tip or at a distance of 0.5 to 2 mm from the notch tip. The infrared

thermography measurements demonstrate that these positions may be within the plastic zone formed during crack initiation [7]. Consequently, deformation of the fracture zone may be due to deformation during crack initiation and crack propagation. The fracture behaviour of the studied blends is described elsewhere [5–7]. In the brittle fracture, the fracture speed is very high ($> 200 \text{ m s}^{-1}$) and the deformation of the material next to the fracture plane is minimal. In ductile fracture the fracture speed is much lower ($< 50 \text{ m s}^{-1}$) and the material next to the fracture plane is strongly deformed. For the blends a weighted average particle (D_w) size is given, defined as: $\sum n_i d_i^2 / \sum n_i d_i$. The D_w particle size correlated well with the T_{bd} [6]. A typical fracture zone of a tough fractured rubber-toughened polypropylene specimen at low test speed (10^{-3} m s^{-1}) is shown in Fig. 3. The dark spots in the micrograph are voids. Round voids are found in the region of 0.1–2 mm from the fracture surface; these voids are randomly distributed. The voids increase in size with their position nearer the fracture surface and have a more elongated shape. The direction of elongation of these voids is in the crack propagation direction. These elongated voids are formed as a result of the strong plastic deformation of surrounding the matrix. The orientation of the elongated voids is illustrated in Fig. 4. The drawn lines in Fig. 4 show the strain direction in the vicinity of a crack tip. Near the fracture surface, the strain direction is parallel to the fracture surface. Far away from the crack, the strain is in the applied force direction. As the stresses around a crack are inhomogeneous, the strains decrease with the distance from the crack.

The layer containing voids is a so-called cavitation layer. The layer containing elongated voids is a deformation layer. The fact that the cavitation layer, in approaching the fracture surface, turns into a deformation layer indicates that the matrix deforms by a yielding mechanism, which is initiated by voided rubber particles. The cavitation layer is probably responsible for diffuse stress whitening as shown in Fig. 2.

The deformation layer is associated with intense stress whitening. This more intense stress whitening in the deformation layer is probably due to the increasing void volume and void dimension. The shape of the intense stress whitening zone (Fig. 2) suggests that the thickness of the cavitation and deformation layer increases with increasing crack length. With increasing temperature the structure of the deformation layer is changed and a melt layer is formed. The fracture zone of a tough broken 70/30 vol% PP–EPDM blend ($D_w = 0.9 \mu\text{m}$) fractured at different test speeds, in the range of 10^{-4} – 10 m s^{-1} , is shown in Fig. 5. At this test temperature the blend has undergone ductile fracture, over the whole test speed range. At low test speed, a clear deformation layer leading up to the fracture surface is observed with a strong elongation of the cavities. At higher test speed ($\geq 0.1 \text{ m s}^{-1}$) the deformation of the cavities seem to be less than at low speeds and a relaxation layer appears. The lower elongation of the cavities might be due to less deformation or relaxation of the blend after fracture. As at these high test

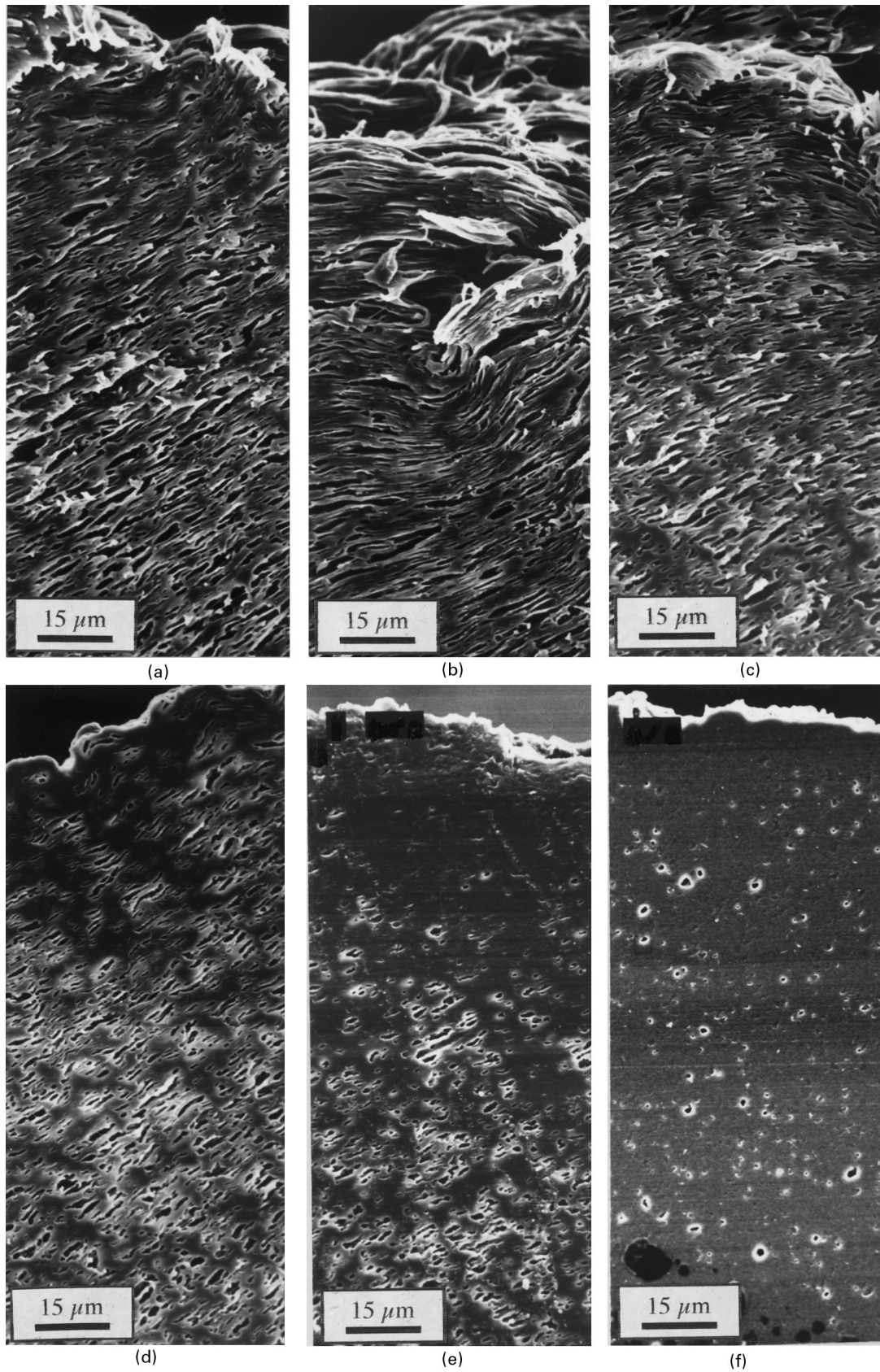


Fig. 5. The fracture of a tough fractured 70/30 vol% PP-EPDM blend ($D_w = 0.9 \mu\text{m}$) at varying test speed and room temperature. Test speed [m s^{-1}]: A: 10^{-4} , B: 10^{-3} , C: 10^{-2} , D: 10^{-1} , E: 0.8, F: 10 Distance to notch: 2 mm. The fracture surface is located at the top, the crack propagates from left to right.

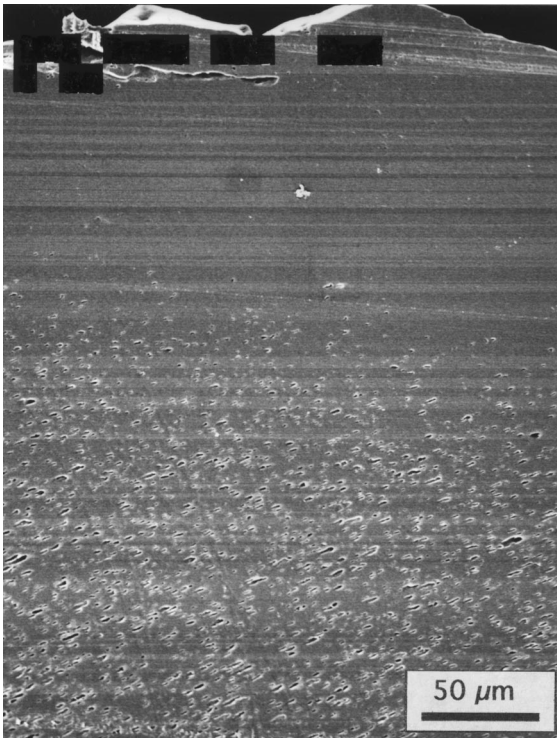


Fig. 6. The fracture zone of a tough fractured 90/10 vol% PP-EPDM blend ($D_w = 0.7 \mu\text{m}$). Test conditions: 1 m s^{-1} and 100°C . Distance to notch tip 2 mm. The fracture surface is located at the top.

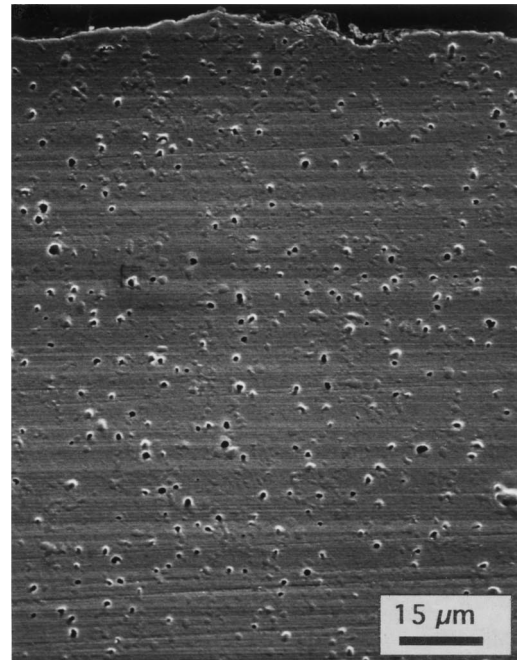
speeds the deformation becomes adiabatic and this is accompanied by a considerable temperature rise [6]. At high temperatures PP becomes elastic and after releasing the stress considerable relaxation can take place resulting in less elongated cavities in the micrographs. The layer without cavities suggest a complete relaxation of the matrix material [9]. At 10 m s^{-1} , only a cavitation layer and a relaxation layer are observed, which suggests that the entire deformation layer has relaxed under the conditions accompanying this very high test speed (high temperature).

The formation of the relaxation layer is accompanied with an increase in fracture energy [6]. The increase in fracture energy is probably due to the crack blunting effect of the relaxation layer. The development of this layer induces a blunting effect.

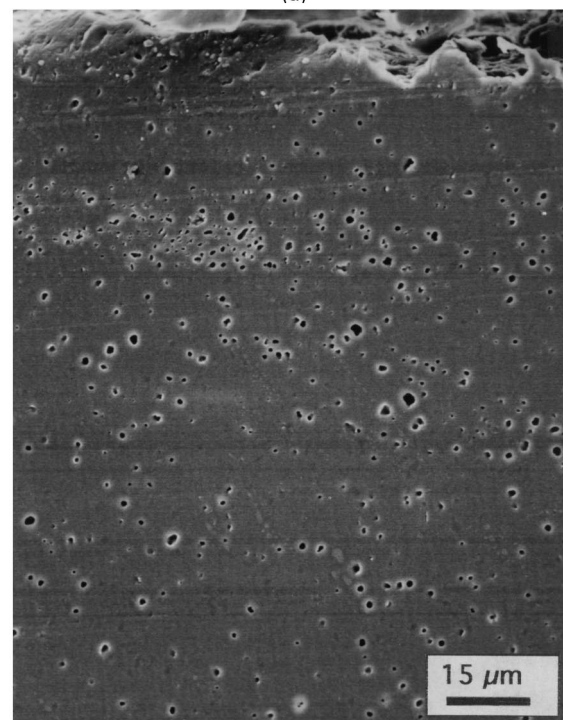
If a samples is tested at high temperature (100°C) and 1 m s^{-1} , the deformation layer is strongly relaxed and the melt layer now has a thickness of $100 \mu\text{m}$ (Fig. 6). At high test temperatures the temperature rise due to adiabatic heating of the deformation and fracture zone is stronger and the relaxation layer is thicker. The relaxation layer, if tested at room temperature and at 2 mm ahead of the notch, is $10\text{--}25 \mu\text{m}$ thick. The relaxation layer of rubber-toughened nylon is thinner ($3\text{--}5 \mu\text{m}$).

3.2. Brittle fracture

The fracture zone of a brittle fractured 70/30 vol%



(a)



(b)

Fig. 7. The fracture zone of a brittle fractured 70/30 vol% PP-EPDM ($D_w = 0.9 \mu\text{m}$) at low and at high test speed. The fracture surface is located at the top. A: 2 mm from the notch tip, test conditions: 10^{-3} m s^{-1} and -50°C . B: At the notch tip, test conditions: 1 m s^{-1} and 0°C .

PP-EPDM blend ($D_w = 0.9 \mu\text{m}$) at low test speed (10^{-3} m s^{-1}) and high test speed (1 m s^{-1}) is shown in Fig. 7. The fracture zone of the corresponding tough fracture is shown in Fig. 5. In the case of brittle fracture, the cavitation layer reaches up to the fracture surface irrespective of

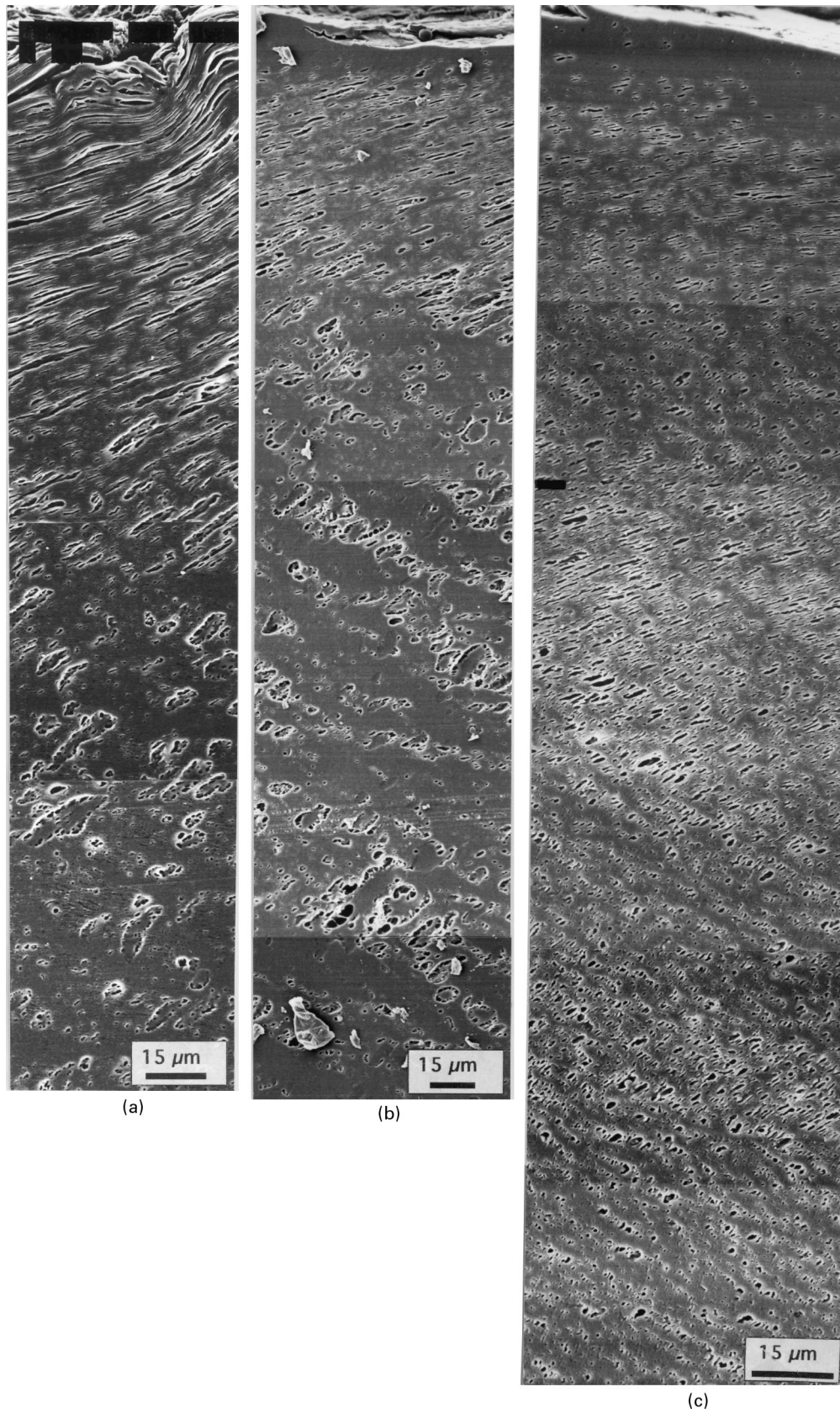


Fig. 8. The fracture zone of a tough fractured 80/20 vol% PP-EPR blend at varying particle size and test speed. Distance to the notch tip: 1 mm. The fracture surface is located at the top, the crack propagates from left to right. A: $D_w = 1.5 \mu\text{m}$, test conditions: 10^{-3} m s^{-1} and -20°C . B: $D_w = 1.5 \mu\text{m}$, test conditions: 1 m s^{-1} and 70°C . C: $D_w = 0.4 \mu\text{m}$, test conditions: 1 m s^{-1} and 70°C .

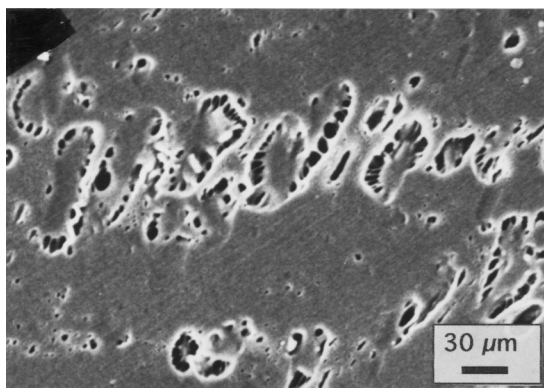


Fig. 9. Cavitated large rubber particles, close-up of Fig. 8B.

the test speed and the deformation and melt layer are not observed. This suggests that during brittle fracture rubber cavitation is taking place but the matrix yielding in-between the cavities is absent.

3.2.1. Particle size

The function of the rubber is to cavitate and this cavitation is expected to depend on the particle size [13]. The larger the particle size the more easy the cavitation is expected to take place. The influence of the particle size is studied on a 20 vol% EPR blends with a ductile fracture (Fig. 8). With a large particle size ($D_w = 1.6 \mu\text{m}$) at low test speed the usual two zone structure is observed. However the cavitation of the large rubber particles proceeds differently from small particles. The large particles contain several cavities situated near the interface with the matrix. At high test speed this blend had now the usual three zone structure and the large particles have cavitated again with several cavities. A close up of such large cavitated particles are given in Fig. 9. The large particles contain several voids and the voids are at the rubber–matrix interface. This was also observed by Chou et al. [8]. Large particles contain several cavitation sites and the conditioning for cavitation is apparently more favourable near the interface than in the centre of a rubber sphere. That in the larger particles several small cavities are formed instead of one large cavity is an advantage, as large cavities are more likely to become unstable. For comparison also a PP–EPR blend is given with small particle sizes ($D_w = 0.4 \mu\text{m}$) deformed at high test speed. This blend has the three-layer structure as we have seen in Fig. 5E.

Based on the structure of the fracture zone of samples tested at high test speeds, it is evident that there is a layer next to the fracture surface which is fully relaxed and a wider zone where there must have been a partly relaxation of the structure. In both blend with the small and the large particle size particles, the matrix deforms by a yielding mechanism which is initiated by cavitated rubber particles. At higher test speed the cavitated particles seem to lie in rows.

3.2.2. Inhomogeneous deformation

In a blend with a small amount of rubber tested at high speed the deformation was found to be in bands (Fig. 10A and B). These bands look like crazes, although their structure is much coarser than that of crazes. The deformation bands seems to initiate cracks, which suggests that they are precursors for fracture. Such an inhomogeneous deformation was not observed at low test speed. With increasing test speed the cavitation is more in layers and thus the deformation more in bands. This test speed effect was also observed in rubber-toughened nylon [5]. The presence of rows suggest an inhomogeneous deformation. This inhomogeneous deformation might be due to inhomogeneous cavitation [14] and/or inhomogeneous matrix deformation before cavitation.

In brittle fracture tested at high speeds sometimes cavity layers can be seen ahead of a branched crack (Fig. 10B and C). Crack branching is takes place at very high fracture speeds ($< 500 \text{ m s}^{-1}$) and can be seen on the fracture surface as ribbons [15].

4. Conclusions

In the PP–rubber blends on brittle fracturing samples, a diffuse stress whitening can be seen. This stress whitening is restricted to the core of the specimen and stretches over the full length of the specimen. This diffuse stress whitened zone contains small cavitated rubber particles. The particles remain small up to the fracture surface. The structure of the fracture zone schematically represented in Fig. 11, layer I.

In the case of tough fracture, next to diffuse stress whitening (layer I) also a triangular zone of intense stress whitening (layer II) is formed next to the fracture plane. The morphology of the intense stress whitened zone is that of cavities which are larger in size and deformed. The deformation of these cavities is smaller if the material is tested at higher speeds and higher temperatures. Both the test speed and the test temperature increases the temperature of the deformation zone. At higher temperatures PP becomes more elastic and stronger elastic recovery after fracture is possible.

At high test speed ($\geq 0.1 \text{ m s}^{-1}$), the deformation layer just beneath the fracture surface has completely relaxed (layer III). In this layer with a thickness of 10–100 μm no cavities can be observed. In the transition from layer II to layer III the cavities already decrease in particle size. The relaxation layer is formed well above 100°C. As the formation of the relaxation layer is accompanied by an increase in fracture energy, the development of this layer induces a blunting effect.

At high test speeds next to the fracture surface, a layer without deformation can be seen and at low test speeds a strongly deformed layer is present. At high test speeds, the temperature is the highest just ahead of the crack tip [7]. Matrix deformation of semi-crystalline polymers do not

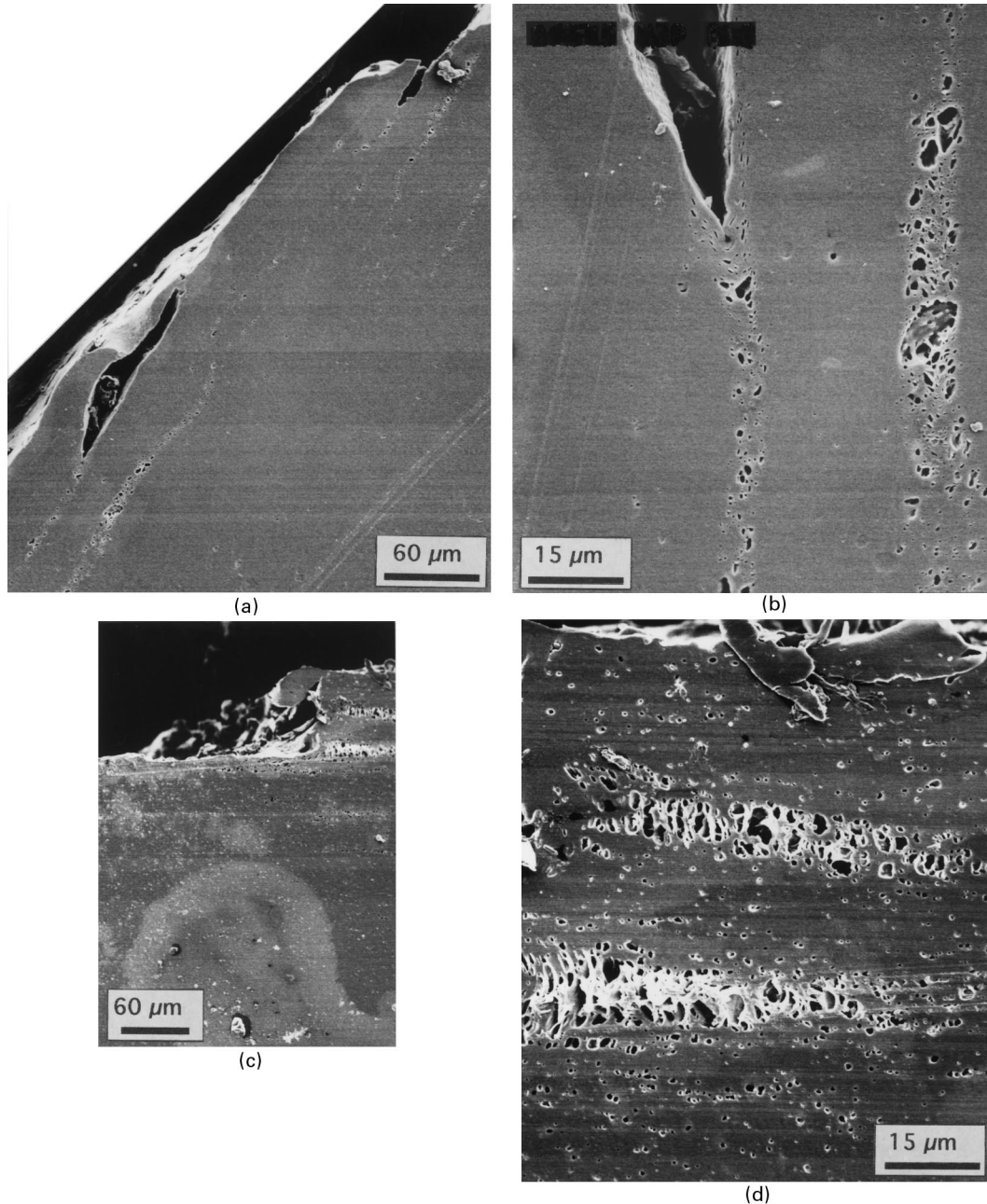


Fig. 10. A: Fracture zone of a tough fractured 95/5 PP-EPR blend ($D_w = 0.8 \mu\text{m}$) test conditions: notched Izod impact test at 61°C . B: Close-up of A. C: Fracture zone of a brittle fractured 90/10 PP-EPDM blend ($D_w = 0.7 \mu\text{m}$), test conditions: 1 m s^{-1} and 60°C . The fracture surface is located at the top. D: Close-up of C.

relax unless very near or above their melting temperature [6]. All these results suggest that ahead of a crack at high test speeds considerable plastic deformation has taken place with a strong temperature rise, a complete relaxation of the matrix material takes place and the rubber particles relax to their original shape.

The cavitation of the rubber particles is, at high test speeds, in rows. This inhomogeneous deformation might be due to an homogeneous cavitation process or due to inhomogeneous matrix deformation before cavitation. This speed effect suggest a temperature effect.

The matrix ahead of the notch deforms by a yielding mechanism, after the rubber particles have voided. In larger particles several voids are present which is an advantage as large voids can more easily initiate fracture. In the studied blends no crazes have been observed, irrespective of the temperature, rubber concentration or particle size.

Acknowledgements

We would like to thank Prof Dr Ir L.C.E. Struik for

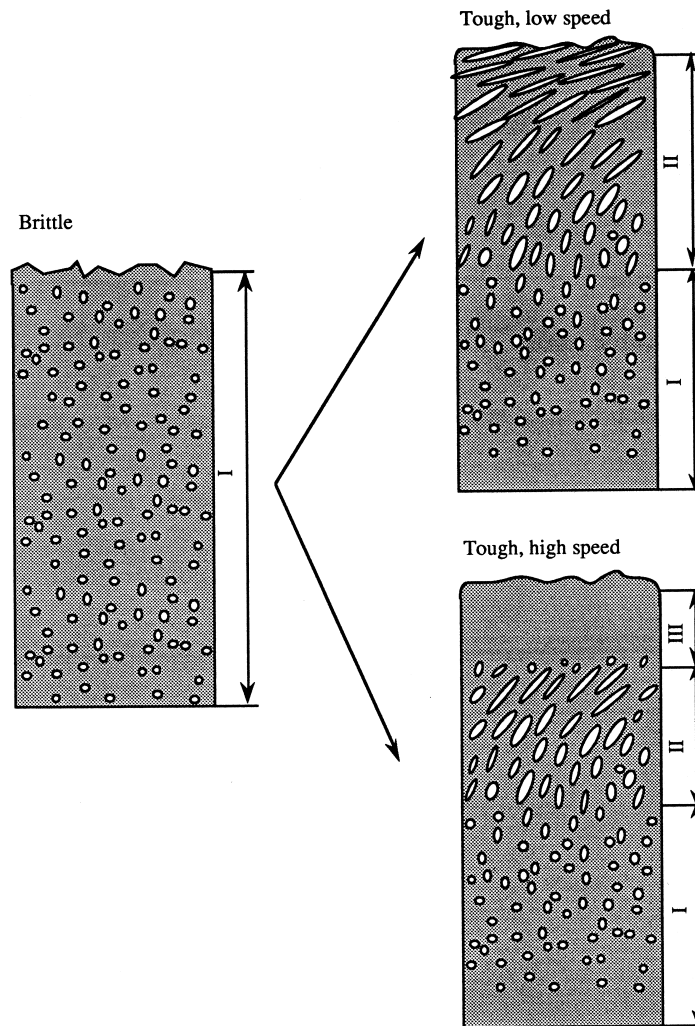


Fig. 11. Schematic representation of the fracture zone of rubber-toughened polypropylene for brittle and tough fracture. The crack propagates from left to right. I: cavitation layer; II: deformation layer; and III: relaxation layer.

helpful discussions and comments and M. Smithers for his contribution concerning the SEM micrographs. This work is part of the research programme of the Twente University.

References

- [1] Ramsteiner F. *Acta Polymerica* 1991;42:584.
- [2] Hayashi K, Morioka T, Toki S. *J Appl Polym Sci* 1993;48:411.
- [3] Jang BZ, Uhlmann DR, Vander Sande JB. *J Appl Polym Sci* 1985;30:2485.
- [4] van der Wal A, Mulder JJ, Oderkerk J, Gaymans RJ. *Polymer* 1998;39:6781.
- [5] van der Wal A, Nijhof R, Gaymans RJ. *Polymer* 1999;40:6031.
- [6] van der Wal A, Gaymans RJ. *Polymer* 1999;40:6045.
- [7] van der Wal A, Verheul AJJ, Gaymans RJ. *Polymer* 1999;40:6057.
- [8] Chou CJ, Vijayan K, Kirby D, Hiltner A, Baer E. *J Mater Sci* 1988;23:2521.
- [9] Dijkstra K, Gaymans RJ. *J Mater Sci* 1994;29:3231.
- [10] Janik H, Gaymans RJ, Dijkstra K. *Polymer* 1995;36:4203.
- [11] Steenbrink AC, Janik H, Gaymans RJ. *J Mat Sci* 1997;32:5505.
- [12] Boode JW, Gaalman AEH, Pijpers AJ, Borggreve RJM. Poster presented at the Prague Macromol. Meetings, 1990.
- [13] Bucknall BC, Karpodinis A, Zhang XC. *J Mat Sci* 1994;29:3377.
- [14] Lazerri A, Bucknall CB. *J Mat Sci* 1993;28:6799.
- [15] Sharon E, Fineberg J. *Phys Rev* 1996;54:7128.